Multiaxial cyclic plasticity model including elastic modulus variation

M Barsanti[1], M Beghini[1], M Loffredo[1], G Macoretta[1], B D Monelli[1,*] and A Bagattini[2]

[1] Dipartimento di Ingegneria Civile e Industriale, University of Pisa, Largo Lazzarino 2, Pisa, Italy
[2] Baker & Hughes Nuovo Pignone, Via Felice Matteucci 2, Florence, Italy

E-mail: michele.barsanti@unipi.it marco.beghini@unipi.it mat.loffredo@gmail.com giuseppe.macoretta@phd.unipi.it bernardo.disma.monelli@unipi.it andrea.bagattini@bakerhughes.com

Abstract. In the present work a multiaxial model is proposed to describe the elastoplastic behaviour of a structural steel in the presence of loading-unloading cycles. The activity is a part of a more estensive research carried out in collaboration with Baker & Hughes aimed at developing an accurate model for accurately predicing residual stresses caused by autofrettage processes in thick cylinders and its experimental verification. It has been demostrated that in order to obtain estimates of the residual stress with errors within a few percent, the constitutive behavior of the material has to be reproduced very accurately. To this purpose, both the Bauschinger effect and the variation of the elastic modulus with the accumulated plastic deformation have to be accurately measured and properly included in the constitutive model.

1. Introduction

The Bauschinger effect occurs in several metallic materials when, after a plastic strain caused, for instance, by tensile stress, the load is reversed and the yielding condition is reached again. The loading and the unloading curves can be very different and the yielding condition in the unloading phase can be attained much earlier. For some materials the effect is so strong that in the unloading phase plastic strains can be produced when the material is still in a tensile condition (see figure 1) thus indicating that the extension of the elastic region is more than halved. For the material under examination, a typical structural steel originally in the quenched and tempered condition, after a plastic strain of a few percent, the yielding strength in the unloading phase $\sigma_y^{(U)}$ is much lower than the inital value $\sigma_y^{(L)}$ measured in the loading phase. Moreover, it is observed that also the shape of the stress-strain curve can be significantly modified as the yielding condition due to the Bauschinger effect is reached more gradually with the material showing a significant increase of the strain-hardening coefficient near the yielding. The variations in yielding strength and the strain hardening coefficient depend on the plastic $\bar{\epsilon}_p$ accumulated during the loading phase.

As the elastic unloading phase is influenced by the Bauschinger effect, a strong reduction in the peak value of the compressive stress produced in the inner wall of the cylinder due to autofrettage (see figure 2) that is one of the most important parameter used to set the autofrettage control parameters [1–3]. The model proposed to reproduce this mechanical behaviour is based on the combination of two effects: an isotropic softening, that accounts for the shrinking of the elastic domain, and a kinematic hardening

* Corresponding author

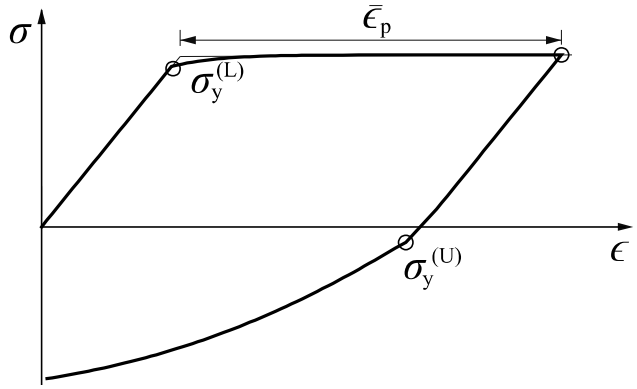

Figure 1. $\sigma - \epsilon$ diagram showing the Bauschinger effect.

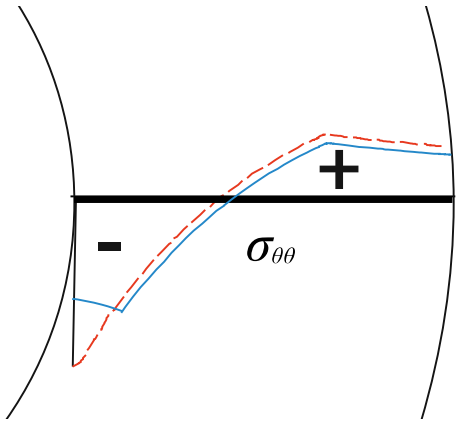

Figure 2. Hoop stress evaluated without (dashed line) and with (solid line) Bauschinger effect.

that properly locates the centre of the elastic locus (back stress tensor). In a preliminary version of this model, presented in [4], the stress-strain relationship was assumed to be defined by a single exponential dependence and the variation of the elastic modulus during the deformation process was neglected. In this paper we present an enhanced version of that model by which the stress-strain curves of the material can be reproduced more accurately.

2. The simplified model

For the reader's convenience, the previous model, fully described in [4], is briefly presented. The elastic properties, Young's modulus E and Poisson ratio ν, were assumed to be not dependent to the plastic strain. The multiaxial plasticity was based on the Von Mises criterion, including kinematic hardening and isotropic softening, with back stress α and radius of yield locus σ_y, as shown in figure 3 [5]. The model was developed to exhibit the following features:

(i) when yielding condition is not verified, the consitutive law must be elastic with the same elastic properties in the loading and in the unloading phases
(ii) the experimentally obtained unixaial stress-strain curve in the loading phase, including the tensile yield point and the hardening behavior, was reproduced by combining non linear kinematic hardening and non linear isotropic softening
(iii) the relation between the uniaxial strain ϵ and the stress σ_y was considered to depend on the maximum tensile equivalent plastic strain $\bar{\epsilon}_p$, in order to account for the reduction of $\sigma_y^{(U)}$, due to tensile plastic strain
(iv) σ_y, after first yielding, was freezed
(v) the strain hardening parameter after reverse yielding (figure 3) was chosen on the bases of $\bar{\epsilon}_p$.
(vi) after reverse yielding all stress-strain curves were assume to be concurrent in the same point despite the initial plastic strain attained in the loading phase
(vii) in case of reloading (not active in the auto frettage), the stress-strain curve was described by closed loop.

The results obtained using this model, already reported in [4] and repeated here for the reader's convenience, are shown in figure 4. It is evident that the hypothesis of the constancy of the slopes in the elastic sections of the unloading phases is not in agreement with the experimental results, especially for the curves corresponding to high values of $\bar{\epsilon}_p$. Moreover, the not linear portion of the stress-strain curves, particularly near the yielding in the unloading phase, are not well described by a single exponential.

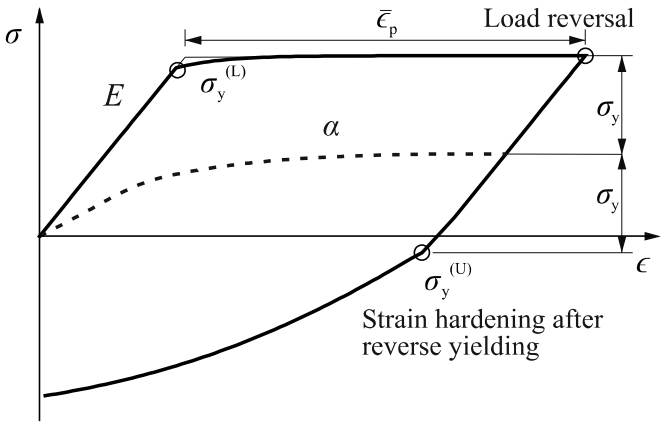

Figure 3. True stress-true strain cycle showing back stress α and radius of yield locus σ_y.

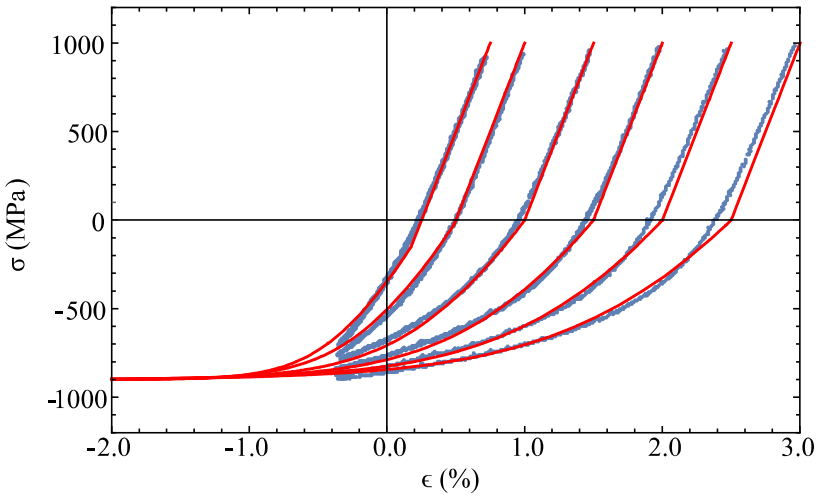

Figure 4. Fit of $\sigma - \epsilon$ experimental data obtained with the simplified model.

3. The improved model

The improvements of the model, object of this work, consisted of the introduction of a sum of exponentials to reproduce more accurately the trend of the constitutive curve and the introduction of a dependence of the elastic modulus on the plastic strain accumulated in the loading phase. In order to take into account the multiaxiality, the Von Mises yield criterion has been adopted for the yielding condition and the associated law has been assumed to accurately reproduce the incremental plastic strain tensor $\boldsymbol{n}$. Equations 1 and 2 have been introduced to describe the kinematic hardening evolution law of the back stress tensor $\boldsymbol{\alpha}^i$:

$$d\boldsymbol{\alpha}^i = C_{1,i}^{(\mathrm{L})}\boldsymbol{n}d\epsilon_\mathrm{p} - C_{2,i}^{(\mathrm{L})}\boldsymbol{\alpha}^i d\epsilon_\mathrm{p} \qquad i = 1 \ldots I \tag{1}$$

$$\alpha_i(\epsilon_\mathrm{p}) = \frac{C_{1,i}^{(\mathrm{L})}}{C_{2,i}^{(\mathrm{L})}}(1 - e^{-C_{2,i}^{(\mathrm{L})}\epsilon_\mathrm{p}}) \qquad i = 1 \ldots I \tag{2}$$

where ϵ_{p} is the equivalent plastic strain and $C_{1,i}^{(\mathrm{L})}$, $C_{2,i}^{(\mathrm{L})}$ are the first and the second parameters (typical of the investigated material) describing kinematic hardening during the loading phases, respectively. Equation 3 has been introduced to take into account the isotropic softening:

$$\sigma_{\mathrm{y}}(\epsilon_{\mathrm{p}}) = \sigma_{\mathrm{y}}^{(\mathrm{L})} + \sum_{j=1}^{J} \frac{H_{1,j}^{(\mathrm{L})}}{H_{2,j}^{(\mathrm{L})}}(1 - e^{-H_{2,j}^{(\mathrm{L})}\epsilon_{\mathrm{p}}}) \tag{3}$$

where $H_{1,j}^{(\mathrm{L})}$ and $H_{2,j}^{(\mathrm{L})}$ are, respectively, the first and the second typical constant of the loading phase isotropic softening. In the previous model presented in [4] it was assumed: $I, J = 1$; the difficulty of the present model lies in the fact that each kinematic model (indexed by i) carries an $\boldsymbol{\alpha}^i$ back stress tensor with its set of parameters. As a consequence, I cannot be increased too much. For each loading cycle, the relationships defining the kinematic hardening and isotropic softening bave been determined evaluating the parameters $C_{1,i}^{(\mathrm{L})}$, $C_{2,i}^{(\mathrm{L})}$, $H_{1,j}^{(\mathrm{L})}$ and $H_{2,j}^{(\mathrm{L})}$ from experimental data. The loading phases have a unique set of parameters, because they are so similar that they can be treated as a single curve.

To take into account the various load reversals, a cycle counter Ω has been introduced, which is increased by 1 at any loading inversion detected by verifying a suitable condition 4 on the scalar product between the plastic flow tensors.

$$\Omega_n = \Omega_{n-1} + 1 \;\; \mathtt{IF}[\mathrm{sign}(\boldsymbol{n}_n \cdot \boldsymbol{n}_{n^*}) = -1] \tag{4}$$

where n^* is the index corresponding to the last plastic iteration, preceeding iteration indexed by n. The kinematic hardening in the unloading phases has been described by equations 5 and 6:

$$d\boldsymbol{\alpha}^i = C_{1,i}^{(\mathrm{U})}\mathbf{n}d\epsilon_{\mathrm{p}} - C_{2,i}^{(\mathrm{U})}(\boldsymbol{\alpha} - \boldsymbol{\beta})d\epsilon_{\mathrm{p}} \tag{5}$$

$$\alpha^i(\epsilon_{\mathrm{p}}) - \beta^i = \frac{C_{1,i}^{(\mathrm{U})}}{C_{2,i}^{(\mathrm{U})}}(1 - \exp(C_{2,i}^{(\mathrm{U})}(\epsilon_{\mathrm{p}} - \bar{\epsilon}_{\mathrm{p}}))) \;\; \mathtt{IF}[\Omega_n \geq 1] \tag{6}$$

In the unloading phases, the parameters $C_{1,i}^{(\mathrm{U})}$, $C_{2,i}^{(\mathrm{U})}$, which are, respectively, the first and the second typical constant of the unloading phase kinematic hardening, have been estimated. The back stress tensor ${\boldsymbol{\beta}^i}_n$ has been introduced (see equation 7) to take into account the memory effects during the inversion phases and which is updated at each load inversion.

$${\boldsymbol{\beta}^i}_n = {\boldsymbol{\alpha}^i}_{n-1} \quad \mathtt{IF}[\Omega_n \neq \Omega_{n-1}] \tag{7}$$

The model parameters describing the unloading phases, needed to describe the investigated material using this model, must be expressed as function of $\bar{\epsilon}_{\mathrm{p}}$ and have been empirically obtained by an accurate fit of several stress-strain curves obtained in uniaxial loading-unloading tests. To take into account the variation of the slope of the curve in the elastic region of the unloading phase, an apparent elastic modulus E^* has been introduced that is a function of the equivalent plastic strain $\bar{\epsilon}_{\mathrm{p}}$ accumulated before the unloading. The variation of the elastic modulus, novelty of this work, has been implemented through the empirical function shown in equation 8.

$$E^*(\bar{\epsilon}_{\mathrm{p}}) = E_0(1 - e^{-CE\bar{\epsilon}_{\mathrm{p}}}) \tag{8}$$

where E_0 is the elastic modulus of the as received material (before the introduction of plastic strains). From the experimental point of view, the estimation of E^* requires refined fit techniques in order to avoid inaccuracies and to estimate the accuracy of the obtained values. Research activities aimed at improving this evaluation are under development.

After estimating the values of the computational plastic deformations, the plastic parameters of the material under consideration can be identified and introduced into an ANSYS model (see equation 9) by adding a dummy temperature effect.

$$\epsilon_{\mathrm{p}}^* - \epsilon_{\mathrm{p}} = \sigma\left(\frac{1}{E} - \frac{1}{E^*}\right) \tag{9}$$

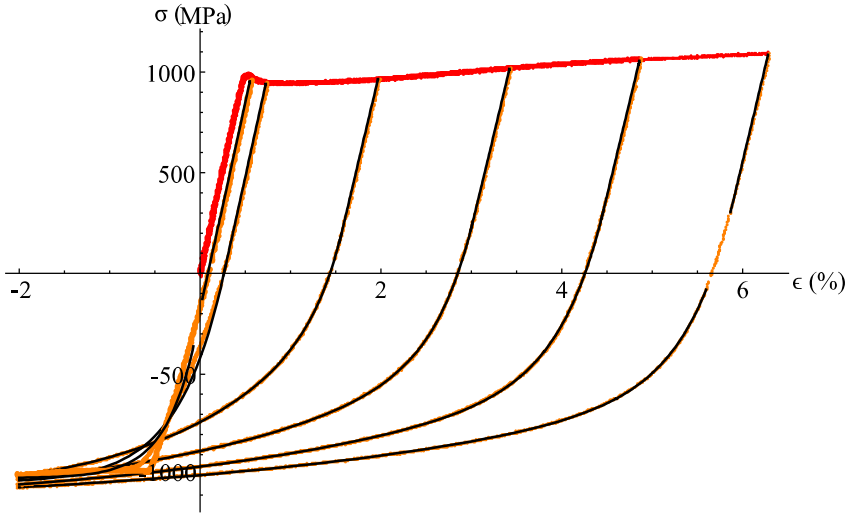

Figure 5. Fit of $\sigma - \epsilon$ experimental data obtained with the enhanced model.

4. Experimental results

Figure 5 shows the unloading phases (in orange the experimentally obtained points) of the stress-strain curves obtained testing AISI 4140 steel specimens. The solid black curves have been obtained using the enhanced model with $I = J = 2$. It can be observed that the improved model reproduces quite accurately the experimentally obtained points, except in the region near the yielding at low initial plastic strain. In order to reproduce the curves in this region, more than two esponential curves should be required. However, in reproducing the autofrettage, the material experiencing that condition is a small portion of the cylinder located rather far form the inner radius and its effect on the peak stress is negligible. A comparison with the results shown in figure 4 evidences that, with a reasonable effort, the interpretation of the experimental data has been considerably improved.

5. The FE model of the autofrettage

To apply the constitutive model to the prediction of residual stresses of an autofrettage cycle, a FE model has been developed using the commercial code ANSYS. The constitutive law has been implemented by means of the User Programmable Features. The implementation of the model was verified by reproducing the uniaxial tests on a single element (see figure 6).

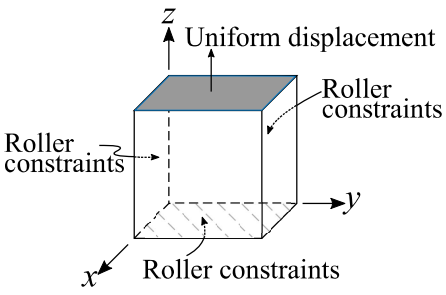

Figure 6. Single FE element.

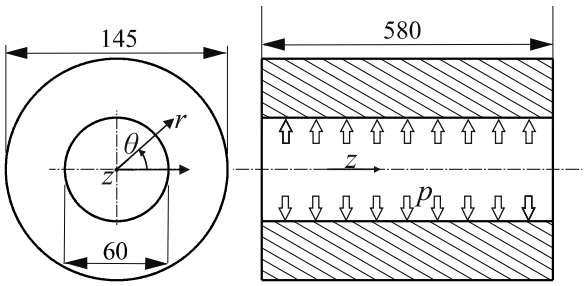

Figure 7. FE model - autofrettaged cylinder ($p = 750$ MPa open-end).

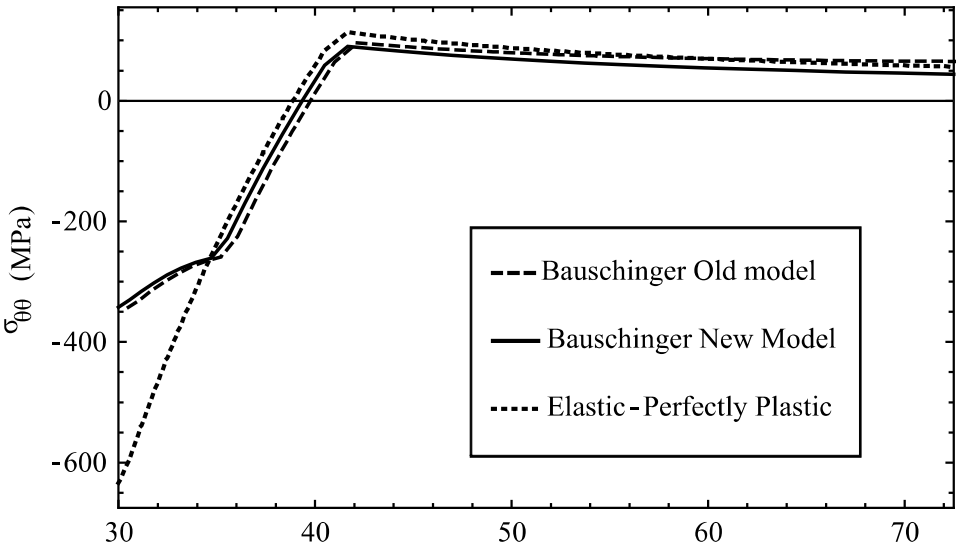

Figure 8. Residual $\sigma_{\theta\theta}$ at cylinder midsection.

6. Application of the FE enhanced model to an autofrettaged cylinder

In order to compare the results of the enhanced model with the ones obtained with the prevous one, an axysimmetric model of the autofrettaged cylinder described in [4]. The internal and external radii are a =30 mm, and b =72.5 mm respectively and the axial length is $L = 4b$. The autofrettage process has been simulated by applying a cycle of internal pressure with the maximum at 750 MPa with both the ends of the cylinder unconstrained (see figure 7). Figure 8 shows the circumferential component of the residual stress (hoop stress) as a function of the distance from the axis in the median section of the cylinder. It can be observed that modelling the Bauschinger effect, even in its most evident effects, produce a strong modification on the estimate of the value of the residual stress at the inner radius. This results was observed also by other authors [6–16].

The differences introduced by the new model in the evaluation of the residual stresses due to the autofrettage are of a few percent. However, the differences can be more significant for other types of geometries, particularly in the presence of notches or when the volume of material experiencing the elastic unloading is more relevant.

7. Conclusions

In the present work, a constitutive model has been that allows an accurate reproduction of the elastic-plastic cyclic behaviour of a typical structural steel is proposed. The model allows for slightly improving the prediction of residual stress in an autofrettage cylinder. The model can be applied to other problems in which the material is subjected to cyclic loads with inversion of the sign of the plastic strain such as in the prediction of the strength or the life of notched components under low cycle fatigue conditions or in the prediction of residual stresses and distortions of metallic sheets after processes involving plastic deformation.

References

[1] Hill R 2009 *The mathematical theory of plasticity* (Oxford: Oxford University Press)
[2] Loffredo M, Bagattini A, Monelli B D and Beghini M 2018 *J. Press. Vessel Technol.* **140** 011402
[3] Beghini M, Loffredo M, Monelli B D and Bagattini A 2018 *Int. J. Pres. Ves. Pip.* **168** 87 – 93
[4] Loffredo M 2018 *Procedia Struct. Integrity* **8** 265 – 75 AIAS2017 - 46th Conference on Stress Analysis and Mechanical Engineering Design, 6-9 September 2017, Pisa, Italy
[5] Auricchio F and Taylor R L 1995 *Int. J. Plast.* **11** 65–98

[6] Chen P C T 1986 *J. Press. Vessel Technol.* **108** 108–12
[7] Livieri P and Lazzarin P 2001 *J. Press. Vessel Technol.* **124** 38–46
[8] Parker A P, O'Hara G P and Underwood J H 2003 *J. Press. Vessel Technol.* **125** 309–14
[9] Parker A P 2000 *J. Press. Vessel Technol.* **123** 271–81
[10] Parker A P, Underwood J H and Kendall D P 1999 *J. Press. Vessel Technol.* **121** 430–7
[11] Parker A P and Underwood J 1998 *Watervliet Arsenal Technical Report* ARCCB–TR–98010
[12] Gibson M C, Hameed A, Parker A P and Hetherington J G 2006 *J. Press. Vessel Technol.* **128** 217–22
[13] Gibson M C, Parker A P, Hameed A and Hetherington J G 2012 *J. Press. Vessel Technol.* **134** 051202
[14] Troiano E, Underwood J H and Parker A P 2006 *J. Press. Vessel Technol.* **128** 185–9
[15] Troiano E, Underwood J H, Venter A M, Izzo J H and Norray J M 2012 *J. Press. Vessel Technol.* **134** 041012
[16] ASME 1997 *Correction for Reverse Yielding (Bauschinger Effect), Pressure Vessel and Piping Design Code* Division 3, Section KD–522.2, p 71